1

# Onboard low-complexity compression of solar images

Shuang Wang, Lijuan Cui, Samuel Cheng, Lina Stanković, Vladimir Stanković

## Abstract

Onboard data processing has always been a challenging and critical task in remote sensing applications due to severe computational limitations of onboard equipment. Satellite images are often rich in content, large in size and dynamic range. Efficient, low-complexity compression solutions are essential to reduce onboard storage, processing, and communication resources. This paper is motivated by recent trends in capturing images from twin satellites, where potential spatial and temporal correlation among the sources can be exploited for more efficient compression. Traditionally, onboard compression tools code images independently without exploiting correlation between different viewpoints. Distributed compression, on the other hand, is a promising technique for onboard coding of solar images since it exploits correlation between different views without compromising the low-complexity and communications requirements of onboard equipment. In this paper we propose an adaptive distributed compression solution using particle filtering that tracks correlation, as well as performing disparity estimation, at the decoder side. The proposed algorithm is tested on the stereo solar images captured by the twin satellites system of NASA's STEREO project. Our experimental results show improved compression performance w.r.t benchmark compression scheme, accurate correlation estimation by our proposed particle-based belief propagation algorithm and significant PSNR improvement over traditional separate bitplane decoding without dynamic correlation and disparity estimation.

## Index Terms

Image compression, Remote sensing, Multiview imaging, Distributed source coding

Shuang Wang, Lijuan Cui, Samuel Cheng are with the School of Electrical and Computer Engineering, University of Oklahoma, Tulsa, OK 74135-2512, USA. Lina Stanković and Vladimir Stanković are with the Dept of Electronic and Electrical Engineering, University of Strathclyde, Glasgow, UK. Tel: ++44-(141)-5482679. E-mail:{shuangwang, lj.cui, samuel.cheng}@ou.edu, {lina, vladimir}.stankovic@eee.strath.ac.uk. This paper will be presented in part at *ICIP-2011 IEEE Intl. Conf. Image Processing,* Brussels, Belgium, Sept. 2011.

## I. INTRODUCTION

Onboard data processing has always been a challenging and critical task in remote sensing applications due to severe computational and/or power limitations of onboard equipment. This is especially the case in deep-space applications, where mission spacecrafts are collecting a vast amount of image data that is stored and/or communicated to the observation center. In such emerging applications, efficient low-complexity image compression is a must. While conventional solutions, such as JPEG, have been successfully used in many prior missions, demand for increasing image volume and resolution as well as increased space resolution and wide-swath imaging calls for a larger coding efficiency at reduced encoding complexity.

NASA's STEREO (Solar TErrestrial RElations Observatory), launched in Oct. 2006, has very recently and still is providing ground-breaking images of the Sun using two space-based observatories [1]. These images aim to reveal the processes in the solar surface (photosphere), through the transition region into the corona and provide the 3D structure of coronal mass ejections (CME). CMEs are violent eruptions solar plasma into space, which, if directed towards the Earth and reaches it as an interplanetary CME along with solar flares of other origin, are known to have catastrophic effects on the radio transmissions, satellites, power grids resulting in large scale and long-lasting power outages, and on humans travelling in airplanes at high altitude.

The data streams that are transmitted 24 hours per day as weather beacon telemetry from each spacecraft have to be heavily compressed [1]. The reconstructed images are available online, immediately after reception. Due to compression, many image artifacts have been spotted that led to wrong conclusions (see e.g., [2]). Another, scientific stream is recorded and transmitted daily using NASA Deep Space Network lightly compressed. These images are becoming available 2-3 days after arrival in the Flexible Image Transport System (FITS) and/or JPEG format.

A variety of image compression tools are currently used in deep-space missions, ranging from Rice and lossy wavelet-based compression tools (used in PICARD mission by CNES2009), Discrete Cosine Transform (DCT) + scalar quantization + Huffman coding (Clementine, NASA1994), ICER (a low-complexity wavelet-based progressive compression algorithm used in Mars mission, NASA2003) to (12-bit) JPEG-baseline (Trace NASA1998, Solar-B JAXA2006) [3]. The compression algorithms have mainly been implemented in hardware (ASIC or FPGA implemen-

tation), but some of them run as software on DSP processors (e.g., ICER). The key characteristics of these algorithms are relatively-low encoding power consumption, coding efficiency, and error resilience features. Latest Earth observation satellites usually employ JPEG2000 [4] or similar wavelet-based bitplane coding methods implemented on FPGA, which might be too prohibitive for deep-space missions. Note that all current missions, including STEREO, use 2D, mono-view image compression trading off computational cost and compression performance. Since STEREO images are essentially multi-view images, with high inter-view correlation, current compression tools do not provide an optimum approach. In this paper, we propose a *distributed multi-view image compression (DMIC) scheme* for such emerging remote sensing setups.

When an encoder can access images from multiple views, a joint coding scheme [5] achieves higher compression performance than schemes with separate coding, since multi-view images are usually highly correlated. However, due to the limited computing and communication power of space imaging systems, it is not feasible to perform high-complexity, power-hungry onboard joint encoding of captured solar images. Although, intuitively, this restriction of separate encoding seems to compromise the compression performance of the system, distributed source coding (DSC) theory [6], [7] proves that distributed independent encoding can be designed as efficiently as joint encoding as long as joint decoding is allowed, propelling DSC as an attractive low-complexity onboard source coding alternative.

The proposed DMIC image codec is characterised by low-complexity image encoding, and relatively more complex decoding meant to be performed on the ground. A novel joint bitplane decoder is described, that integrates particle filtering with standard Belief Propagation (BP) decoding to perform inference on a single joint 2-D factor graph. We test our lossy DMIC setup with grayscale stereo solar images obtained from NASA's STEREO mission [1] to demonstrate high compression efficiency with low encoding complexity and non power-hungry onboard encoding, brought about by DSC. DSC has been used for onboard compression of multispectral and hyperspectral images in [8], [9], where DSC is used to exploit efficiently inter-band correlation. In [9], for example, a low-complexity solution robust to errors is proposed using scalar coset codes to encode the current band and the previous bands as decoder side information. The algorithms of [9] are implemented using FPGA, and simulations on AVIRIS images show promising results.

The key contributions of this paper can be summarised as:

- An adaptive distributed multi-view image decoding scheme, which can estimate the block-

wise correlation and disparity change between two correlated images, and also recover the images simultaneously;

- A BP decoder with integrated particle filtering to estimate blockwise correlation changes, since standard BP cannot handle continuous variables (except linear Gaussian model) such as the correlation parameter. This extends our previous work [10], [11] from 1-D correlation estimation to 2-D and from time varying correlation estimation to spatial varying correlation estimation;

- A joint bitplane decoder (compared to the traditional separate bitplane decoder [12]), that allows the estimation of the correlation and the disparity between two pixels directly rather than just the correlation between a corresponding pair of bits of the pixels;

- A decoding scheme that offers greater feasibility for rate selection than the joint bitplane encoder/decoder design used in [13] since the received syndromes of each bitplane are independent due to separate bitplane encoding.

This paper is organized as follows. Section II gives the relevant background on distributed compression of correlated sources with independent encoding and joint decoding, including prior work on distributed multi-view image coding. We describe the DMIC setup in Section III and our proposed adaptive DMIC algorithm, which includes the disparity and the correlation estimation in Section IV. Experimental results are described in Section V. Section VI concludes the paper.

## II. BACKGROUND

### A. Distributed Source Coding (DSC)

In a nutshell, DSC refers to separate compression and joint decompression of mutually correlated sources. The sources are encoded independently (hence distributed) at the encoders and decompressed jointly at the decoder. DSC is thus a compression method that aims at exploiting mutual dependencies across different sources that need not communicate among each other.

DSC appeared as an information-theoretical problem in the seminal paper of Slepian and Wolf in 1973 [6]. Slepian and Wolf [6] considered the simplest case of DSC with two discrete sources $X$ and $Y$ and lossless compression, and showed that it is possible to have no performance loss of independent encoding compared to the case when joint encoding is done. Indeed, Slepian and Wolf showed that two discrete sources $X$ and $Y$ can be losslessly decoded as long as:

$$R_X \geq H(X|Y), R_Y \geq H(Y|X), R = R_X + R_Y \geq H(X,Y), \tag{1}$$

where $R_X$ and $R_Y$ are rates used for compressing $X$ and $Y$, respectively. The above set of equations, known as the Slepian-Wolf (SW) coding region, shows that the sum-rate $R$ can be as low as the joint entropy of the sources, which is the same as if the source were encoded together. A special case of SW coding is when one source, e.g., $Y$, is known at the decoder. Then, a rate not higher than $H(X|Y)$ suffices for compressing $X$. This case is known as asymmetric SW coding, or SW coding with decoder side information $Y$.

Practical SW coding is done via conventional channel coding. Indeed, correlation between the sources is seen as a virtual communication channel, and as long as this virtual channel can be modelled by some standard communication channel, e.g., Gaussian, channel codes can be effectively employed.

In 1976, Wyner and Ziv [7] considered a lossy version, with a distortion constraint, of the asymmetric SW coding problem and showed that for a particular correlation where source and side information are jointly Gaussian, there is no performance loss due to the absence of side information at the encoder.

Wyner-Ziv (WZ) source coding is usually realized by quantization followed by SW coding of quantization indices based on channel coding [14]. Quantization is used to tune rate-distortion performance, while the SW coder is essentially a conditional entropy coder. The WZ decoder will thus comprise an SW decoder, which makes use of side information to recover the coded information. The SW decoder is followed by a minimum-distortion reconstruction of the source using side information. With WZ coding, side information is not needed at the encoder. The latest designs based on quantization followed by advanced channel coding come very close to the theoretical bounds (see, e.g., [15], [16]).

In much the same way as the information-theoretical DSC framework [6], [7], the state-of-the-art SW and WZ code designs based on advanced turbo and low-density parity-check (LDPC) codes perform well only when correlation statistics between sources are stationary and known at the encoder and decoder. The problem of accurate statistical correlation estimation between the source and side information is particularly important in WZ coding, since there is no unique correlation model for non-stationary (temporal and/or spatial varying) sources.

*B. Related Work*

Since our proposed DMIC scheme intersects several research topics, we group prior work into three categories.

The first category relates to work in the area of low-complexity onboard/remote multi-view image coding. This area is still in its infancy and we found only two relevant contributions. In [17], lossy compression of Earth orbital stereo imagery used for height detection with three or four views based on motion compensation and JPEG-2000 [4] and JPEG-LS is proposed. Note that motion compensation+ JPEG-2000 might still be considered as power expensive for remote sensing, including deep-space missions. In [18], a modification of the mono-view ICER image coder, employed in the Mars Exploration mission, is proposed. The proposed coder optimizes a novel distortion metric that reflects better stereoscopic effects rather than conventional mean-square error (MSE) distortion. The results reported in [18] show improved stereo ranging quality despite the fact that correlation information between the left and right image pair was not exploited in any way or form. See also [19].

The second relevant topic is correlation tracking in DSC applications. Most DSC designs, including Distributed Video Coding (DVC), so far (with few exceptions) usually simplify the problem by modeling correlation noise, i.e., the difference between the source and side infor-mation, as Laplacian random variables and estimate the distribution parameters either based on training sequences or previously decoded data. This imposes certain loss especially for images or sequences that are very different or non-stationary. Non-stationarity of the scene has been dealt mainly by estimating correlation noise (e.g., on the pixel or block level) from previously decoded data and different initial reliability is assigned to different pixels based on the amount of noise estimated both in pixel- and transform-domains [20]–[24]. In [11], we proposed an efficient way of estimating correlation between the source and side information for pixel-domain DVC by tightly incorporating the process within the SW decoder via SW code factor graph augmentation to include correlation variable nodes with particles such that particle filtering is performed jointly with BP over the augmented factor graph during the SW decoding process. Note that the BP-based SW decoding and correlation statistics estimation are considered jointly. The proposed correlation estimation design was tested on a transform-domain DVC [25] with a feedback channel, but with joint bit-plane coding. This work extends this result from mono-view

to low-encoding complexity multi-view coding.

The third relevant topic is multi-view image coding using DSC principles. Despite the potential of DSC, attaining its ultimate performance relies on the assumption that both the correlation and the disparity among multi-view images are known a *priori* at the decoder. Direct measurement of the correlation and the disparity at the encoder side is both expensive in terms of computation and impossible without communication among imaging sensors. Thus, estimating correlation and disparity at the decoder becomes the main challenge in DMIC. For disparity estimation in DMIC, the idea of motion compensation [26], [27] used in DVC offers a possible solution. However, these motion compensation methods usually require excessive amount of computation. Thus, some low complexity disparity learning schemes for DMIC have been proposed in the literature. In [13], Varodayan *et. al.* developed an Expectation Maximization (EM) based algorithm at decoder to learn block-based disparity for lossless compression [13] and then extended it to lossy case [28]. In comparison with the system without disparity compensation, a better compression performance is observed when disparity compensation is employed at the decoder [13], [28].

Thus, knowing the correlation among multi-view images is a key factor in determining the performance of a DMIC scheme. This correlation is generally nonstationary (spatially varying) and should be handled adaptively. For example, in [29] an edge-based correlation assignment method is proposed, where the correlation parameters of blocks with and without edges are assigned to different values. However, even the aforementioned work is based on the assumption that the correlation among images is known a *priori*. Similarly to disparity compensation, dynamic correlation estimation given at the decoder could also yield significant improvement in performance. However, most studies of correlation estimation in DSC focus on the correlation estimation of stationary binary sources [30], [31], which are not suitable for the non-binary image sources in the DMIC case.

Several other approaches were proposed in literature [32]–[35], neither of which uses correlation tracking. A review on multiview-video coding based on DSC principles can be found in [36], [37].

### III. DISTRIBUTED MULTI-VIEW IMAGE CODING: SYSTEM SETUP

The block diagram of the proposed DMIC system is shown in Fig. 1. Two cameras capture the same scene from two different angles. The captured images need to be compressed under
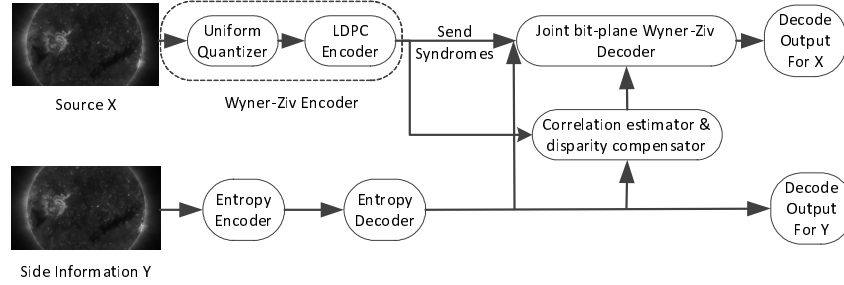
Fig. 1.   Lossy DMIC setup with disparity and correlation estimation.

a distortion constraint independently and communicated to the ground station for processing. Since the two cameras view the same scene only from different angles the images captured at the cameras are mutually correlated. The decoder at the ground station exploits this correlation and both compressed sources to jointly decompress them. The two decompressed images can then be used to generate a 3D image of the scene.

Let $X$ and $Y$ be a pair of correlated multi-view images with size $M$ by $N$ pixels. Assuming that a horizontal disparity shift $D$ exists between pixels of $X$ and pixels of $Y$, the relationship between $X$ and $Y$ can be modeled as

$$X_{(x,y)} = Y_{\left(x - D_{(x,y)}, y\right)} + Z_{(x,y)}, \tag{2}$$

where $x = 1, 2, \ldots, M$ and $y = 1, 2, \ldots, N$ denote the coordinates of pixels, and $Z_{(x,y)}$ satisfies a zero mean Laplace distribution $\mathcal{L}(Z_{(x,y)}|\sigma) = \frac{1}{2\sigma}\exp\left(-\frac{|Z_{(x,y)}|}{\sigma}\right)$.

We consider a lossy asymmetric DMIC setup as shown in Fig. 1, where image $Y$, the side information, is known at the decoder through a conventional image coding. Then, the task is to compress $X$ as close as possible to the WZ bound [7]. At the encoder side, image $X$ is first quantized into $Q[X_{(x,y)}]$ using $2^q$ level uniform nested scalar quantization (NSQ) [38] and then is SW encoded using LDPC codes [12], where each bit-plane is independently encoded into syndrome bits of an LDPC code. Denote $X^1_{(x,y)}, X^2_{(x,y)}, \ldots, X^q_{(x,y)}$ as the binary format of the index $Q[X_{(x,y)}]$, and denote $\mathbf{B^j} = X^j_{(1,1)}, X^j_{(1,2)}, \ldots, X^j_{(M,N)}$ as the $j^{th}$ significant bit-plane, where the superscript $j = 1, \ldots, q$ is used to represent the $j^{th}$ quantized bit or the $j^{th}$ bit-plane in the rest of this paper.

Syndrome bits are sent to the ground station via noiseless channel. The BP algorithm is employed to decode image $X$ using the received syndrome bits, the given correlation between
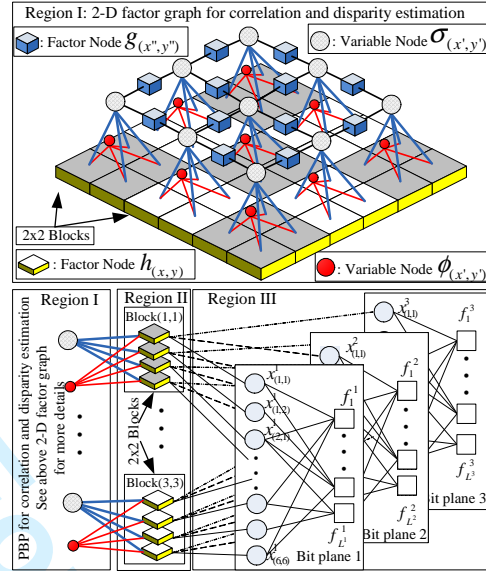
Fig. 2.   Factor graph of joint bit-plane decoder with disparity and correlation estimation.

$X$ and $Y$, and the side information $Y$ reordered by the given disparity information by the station's LDPC decoder. Finally, when the BP algorithm converges, image $X$ can be recovered based on the output belief for each pixel [12].

Note that this asymmetric setup can easily be extended to the non-asymmetric one using, e.g., time-sharing or channel code partitioning [39]. This way, the rate between the two cameras can be traded off.

## IV. ADAPTIVE JOINT BIT-PLANE WYNER-ZIV (WZ) DECODING OF MULTI-VIEW IMAGES WITH DISPARITY ESTIMATION

### A. Joint Bit-plane WZ Decoding

In popular layer WZ approaches such as [12], each bit-plane of the quantized source is recovered *sequentially* and this makes it difficult and inefficient for the decoder to perform the disparity and correlation estimation. In order to facilitate this process, we introduce a joint bit-plane WZ decoding scheme, which can adaptively exploit the disparity and the correlation between a non-binary source and side information during the decoding process. The main idea of our proposed joint bit-plane WZ decoding scheme is illustrated in Regions II and III of the augmented decoder factor graph shown in Fig. 2, where all circle nodes denote variable

nodes and all square nodes denote factor nodes. The encoder used in this paper is the traditional syndrome-based approach using LDPC codes [12], where a given bit plane $\mathbf{B^j}$ is compressed into $L^j$ number of syndrome bits, $\mathbf{S^j} = s_1^j, s_2^j \ldots, s_{L^j}^j$, thus resulting in $(M \times N) : L^j$ compression.

At the joint bit-plane decoder, the factor nodes $f_1^j, f_2^j \ldots, f_{L^j}^j$ as shown in Region III of Fig. 2, take into account the constraint imposed by the received syndrome bits. For a factor node $f_a^j, a = 1, \ldots, L^j, j = 1, \ldots, q$, we define the corresponding factor function as

$$f_a^j(\tilde{\mathbf{X}}_a^j, s_a^j) = \begin{cases} 1, & \text{if } s_a^j \oplus \bigoplus \tilde{\mathbf{X}}_a^j = 0, \\ 0, & \text{otherwise.} \end{cases} \tag{3}$$

where $\tilde{\mathbf{X}}_a^j$ denotes the set of neighbors of the factor node $f_a^j$, $\oplus$ represents the bitwise addition and $\bigoplus \tilde{\mathbf{X}}_a^j$ denotes the bitwise sum of all elements of the set $\tilde{\mathbf{X}}_a^j$.

Then in Region II, the relationship among a candidate quantized source $Q[X_{(x,y)}]$, side information $Y_{(x,y)}$ and disparity compensation $D_{(x,y)}$ can be modeled by the factor function

$$h_{(x,y)}(Q[X_{(x,y)}], Y_{(x,y)}, \sigma, D_{(x,y)}) = \int_{P(Q[X_{(x,y)}])}^{P(Q[X_{(x,y)}]+1)} \frac{1}{2\sigma} \exp\left(-\frac{|\mathcal{X} - Y_{(x-D_{(x,y)},y)}|}{\sigma}\right) d\mathcal{X}, \tag{4}$$

where $P(\mathcal{Q})$ denotes the lower boundary of quantization partition at index "$\mathcal{Q}$", e.g., if a pixel $X_{(x,y)}$ satisfies $P(\mathcal{Q}) \leq X_{(x,y)} < P(\mathcal{Q}+1)$, the quantization index $Q[X_{(x,y)}]$ of pixel $X_{(x,y)}$ is equal to "$\mathcal{Q}$". Then, given the estimation of the correlation $\sigma$ and the disparity $D_{(x,y)}$, standard BP can be used to perform joint bit-plane decoding based on the proposed factor graph (see Regions II and III in Fig. 2) and the corresponding factor functions (3) and (4).

### B. Adaptive Joint Bit-plane WZ Decoding with Disparity Estimation

We assume that each block includes $n \times n$ pixels and shares the same disparity, which yields $\left\lceil \frac{M}{n} \right\rceil \times \left\lceil \frac{N}{n} \right\rceil$ number of blocks for an $M \times N$ image, where $\lceil \bullet \rceil$ represents the ceiling of "$\bullet$" that rounds "$\bullet$" towards positive infinity. Then the horizontal disparity field is a constant within a block and will be denoted as $D_{(x',y')} \in \{-l, \cdots, 0, \cdots, l\}$, where $x' = 1, \cdots, \left\lceil \frac{M}{n} \right\rceil$ and $y' = 1, \cdots, \left\lceil \frac{N}{n} \right\rceil$ are the block indices. Thus, in the rest of this paper, we will use $D_{(x',y')}$ to represent the disparity $D_{(x,y)}$ of a pixel $X_{(x,y)}$ that lies inside the Block$(x', y')$. For example, in the 2-D factor graph of Fig. 2, a $6 \times 6$ image is divided into $3 \times 3$ number of blocks with $2 \times 2$ pixels in each block.

In order to estimate the disparity between images, we introduce extra variable nodes $\phi_{(x',y')}$ in Region I (see the 2-D factor graph in Fig. 2). Each factor node $h_{(x,y)}$ in Region II is connected

11

$$m_{h_{(x,y)} \to \phi_{(x',y')}} \left( D_{(x',y')} \right) \propto \sum_{Q[X_{(x,y)}] \in [0,2^q]} h_{(x,y)}(Q[X_{(x,y)}], Y_{(x,y)}, \sigma, D_{(x',y')}) \prod_{j=1}^{q} m_{X_{(x,y)}^j \to \phi_{(x',y')}} \left( X_{(x,y)}^j \right) \quad , \quad (5)$$

$$m_{h_{(x,y)} \to X_{(x,y)}^j} \left( X_{(x,y)}^j \right) \propto \sum_{D_{(x',y')}} h_{(x,y)}(Q[X_{(x,y)}], Y_{(x,y)}, \sigma, D_{(x',y')}) m_{\phi_{(x',y')} \to h_{(x,y)}} \left( D_{(x',y')} \right) \prod_{j' \in [1,q]/j} m_{X_{(x,y)}^{j'} \to h_{(x,y)}} \left( X_{(x,y)}^{j'} \right) ,$$

(6)

to an additional variable node $\phi_{(x',y')}$ in Region I. Here we define the connection ratio as the number of factor nodes $h_{(x,y)}$ in Region II which each variable node $\phi_{(x',y')}$ is connected to, e.g., the connection ratio is equal to 4 in Fig. 2. According to the BP update rules, the factor node update from Region II to the variable node $\phi_{(x',y')}$ in Region I can be written as (5), where $\mathcal{N}(\phi_{(x',y')})/h_{(x,y)}$ denotes all the neighboring factor nodes of variable node $\phi_{(x',y')}$ except $h_{(x,y)}$. Moreover, (5) can be seen as the E-step algorithm used in [13]. Similarly, the factor node update from Region II to Region III can be written as (6), where (6) can also be seen as the M-step algorithm used in [13]. Thus our approach provides a unified framework that is easier to be understood and be implemented.

## C. Adaptive Joint Bit-plane WZ Decoding with Correlation Estimation

To compress image $X$ close to the WZ bound in the standard BP approach, the correlation parameter $\sigma$ must be known a *priori*. However, in practice, the correlation between the colocated pixels of the pair of correlated images $X$ and $Y$ is unknown, and making the situation even more challenging, this correlation may vary over space. Thus, besides the proposed disparity estimation, we introduce an additional correlation estimation algorithm to perform online correlation tracking by extending our previous correlation estimation model [10] from 1-D to 2-D and from time-varying to spatially-varying. Moreover, our proposed framework is universal and can be applied to any parametric correlation model.

Namely, we assume that $\sigma$ is unknown and varies block-by-block over space, where the same blockwise assumption is also used in Section IV-B. To model this, we introduce another set of extra variable nodes $\sigma_{(x',y')}$ in Region I (see the 2-D factor graph in Fig. 2). Now, each factor node $h_{(x,y)}$ in Region II will be connected to an additional variable node $\sigma_{(x',y')}$ in Region I. Here the connection ratio used for correlation estimation is the same as that for disparity estimation in Section IV-B. Moreover, the correlation parameter $\sigma$ used in the factor function

12

$h_{x,y}(Q[X_{(x,y)}], Y_{(x,y)}, \sigma, D_{(x',y')})$ can be modified accordingly by replacing $\sigma$ as $\sigma_{(x',y')}$, since we assume $\sigma$ varies over space.

Furthermore, the correlation changes among adjacent blocks may not be arbitrary [29]. The ability to capture correlation changes among adjacent blocks can significantly increase the stability of correlation tracking of each block. To achieve this, we introduce additional factor nodes $g_{(x'',y'')}$ in Region I (see the 2-D factor graph in Fig. 2), where $x'' = 1, \cdots, \lceil \frac{M}{n} \rceil - 1$ and $y'' = 1, \cdots, \lceil \frac{N}{n} \rceil - 1$ denote block indices just as $x'$ and $y'$. The corresponding factor function can then be modeled as

$$g_{(x'',y'')}\left(\sigma_{(x'',y'')}, \sigma_{(x''+c,y''+d)}\right) = \exp\left(-\frac{\left(\sigma_{(x'',y'')} - \sigma_{(x''+c,y''+d)}\right)^2}{\lambda}\right) \tag{7}$$

where the offset $(c, d)$ is restricted to $\{(0,1),(0,-1),(1,0),(-1,0)\}$ according to the defined 2-D factor graph, and $\lambda$ is a hyper-prior and can be chosen rather arbitrarily.

Since standard BP can only handle discrete variables with small alphabet sizes or continuous variables with a linear Gaussian model, it cannot be applied directly for estimating the continuous correlation parameters. However, by incorporating particle filtering with BP, we are able to extend BP to handle continuous variables. Then the proposed factor graph model can be used to estimate the continuous correlation. Due to space limitations, we direct readers to our prior work [10] for more details on the particle-based BP (PBP) implementation.

## V. RESULTS

To verify the effect of correlation and disparity tracking for DMIC, we test the above setup with grayscale stereo solar images [1] captured by two satellites of the NASA's STEREO project, where the twin satellites are about 30 million miles apart, and the viewing angle is about $6 - 8$ degrees. For the purposes of illustrating accurate tracking of the correlation and the disparity, our simulations for the SW code use only a low-complexity regular LDPC code with variable node degree 5. More complex irregular codes would further improve the overall peak signal-to-noise ratio (PSNR) performance.

The following constant parameters are used in our simulations: maximum horizontal shift $l = 5$, block size $n = 4$, hyper-prior $\lambda = 10$, initial correlation for Laplace distribution $\sigma = 5$
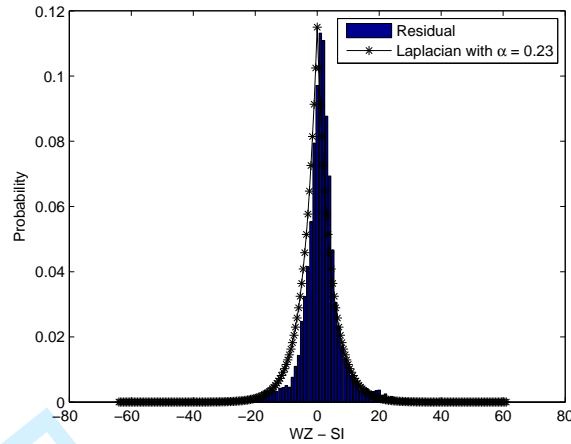
Fig. 3.    Residual histogram for solar images in SET 1.

and initial distribution of disparity

$$p(D_{(x',y')}) = \begin{cases} 0.75, & \text{if } D_{(x',y')} = 0; \\ 0.025, & \text{otherwise}; \end{cases},$$

where the selection of initial values follows [13]. Moreover, we present results for two sets of solar images referred to as solar image SET 1 and solar image SET 2. All tested images are of size $M \times N = 128 \times 72$ pixels.

First, we verify the Laplacian assumption of the correlation between correlated images $X$ and $Y$ in Fig. 3. The x-axis in the figure shows the pixel difference between image $X$ and side information $Y$, while on the y-axis probability of occurrence of such difference in shown. A solid line shows an approximation with Laplacian parameter $\alpha$ set to $0.23$. Obviously, Laplace distribution provides a good starting approximate to the residual between images $X$ and $Y$.

Then, we examine the rate-distortion performance of the proposed adaptive DMIC scheme, where PSNR of the reconstructed image is calculated as an indicator of the distortion. We consider the following five different schemes.

a). Adaptive correlation DMIC with a known disparity, which is used as the benchmark performance.

b). Adaptive correlation and disparity DMIC, which is the proposed scheme in this paper.

c). Adaptive disparity DMIC with a known fixed correlation, which corresponds to the setup used in [13], [28].

14

d). Non-adaptive joint bit-plane DMIC with known fixed correlation only, where the correlation and disparity estimators are not available at the decoder.

e). Non-adaptive separate bit-plane DMIC with known fixed correlation only, which corresponds to the setup used in [12].

Results for solar images in SET 1 and SET 2 are given in Fig. 4 and Fig. 5, respectively. The results are shown as compression rate vs. PSNR of he reconstruction. As expected, the benchmark setup in case a) shows the best rate-distortion performance, since the reference disparity is known before decoding. Comparing cases b) and c), we find a significant performance gain of the proposed scheme b) due to the improved knowledge of correlation statistics due to dynamic estimation. Moreover, all the adaptive DMIC schemes (cases a), b) and c)) outperform the non-adaptive schemes (cases d) and e)). Besides, in the case without adaptive decoding, we find that the performance of joint bit-plane DMIC in case d) is still better than separate bit-plane DMIC in case e). One possible reason for this is that the joint bit-plane DMIC in case d) can exploit the correlation between two non-binary sources much better, since in case e), each bit-plane is decoded separately.

The performance of JPEG codec and JPEG2000 codec are also shown as references in Fig. 4 and Fig. 5. One can see that DMIC schemes significantly outperform two independent JPEG codings, while JPEG2000 is still unreachable due to its high compression efficiency and used arithmetic entropy coding at the cost of high encoding complexity.

Finally, Fig. 6 and Fig. 7 show the final estimate of the correlation and the disparity for solar images in SET 1 and SET 2, respectively, where the reference disparity and residual after $4 \times 4$ block matching between source and side information are provided as references. We can see that the proposed adaptive DMIC scheme outputs a good estimate for both correlation and disparity. This also explains why the rate-distortion performance of adaptive decoding outperforms the non-adaptive decoding scheme in Fig. 4 and Fig. 5.

## VI. CONCLUSION

This paper is motivated by the limited onboard processing and communications requirements of correlated images captured by different telescopes or satellites. Traditionally, these images are compressed independently using state-of-the-art, low-complexity compression algorithms such as
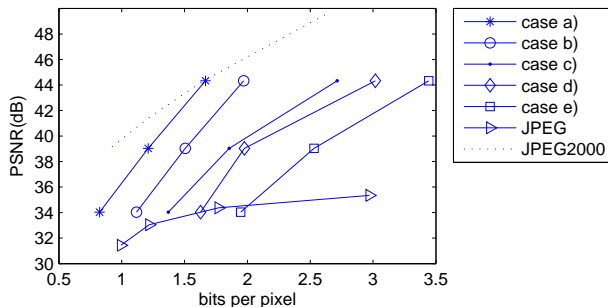
Fig. 4. Rate-distortion performance of the proposed adaptive DMIC scheme for solar images in SET 1.
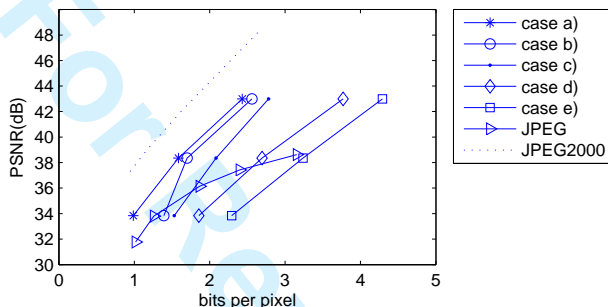


Fig. 5. Rate-distortion performance of the proposed adaptive DMIC scheme for solar images in SET 2.
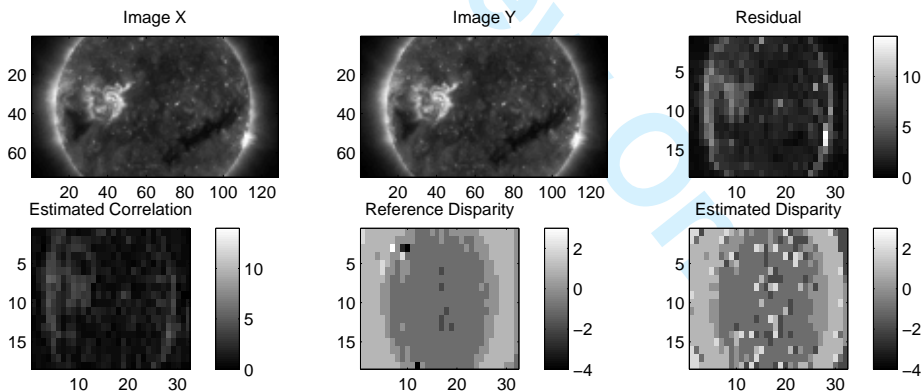


Fig. 6. The final estimate of the correlation and the disparity for solar images in SET 1, where the true disparity and residual after $4 \times 4$ block matching between source and side information are provided as references.

JPEG without considering the spatial and temporal correlation among images captured by deep-space satellites. In order to exploit the correlation among the multiple views acquired from a solar event and enhance compression without jeopardising the encoding onboard complexity and independent encoding process to minimise communication complexity, we proposed an adaptive

16
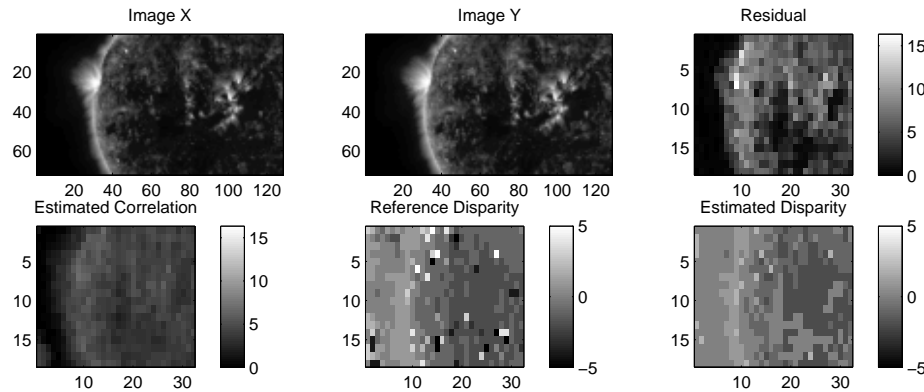


Fig. 7.  The final estimate of the correlation and the disparity for solar images in SET 2, where the true disparity and residual after $4 \times 4$ block matching between source and side information are provided as references.

DMIC algorithm, which can estimate the correlation and disparity between stereo images, and decode image sources simultaneously. To handle spatially-varying correlation between stereo images, we extend our previous particle-based belief propagation work [10] for correlation estimation to the 2-D case. Moreover, our correlation and disparity estimation algorithms are all based on an augmented factor graph, which offers great flexibility for problem modeling in remote sensing applications. Through the results, a significant decoding performance gain has been observed by using the proposed adaptive scheme, when comparing with the non-adaptive decoding scheme and traditional JPEG. While our proposed scheme performs worse than JPEG2000, the latter has significantly higher encoding complexity comparing to ours.

## REFERENCES

[1] http://www.nasa.gov/mission_pages/stereo/mission/index.html.

[2] "http://24sevenpost.com/paranormal/ufo-spotted-visiting-sun-nasa-image," *Accessed May 17th, 2011*.

[3] G. Yua, T. Vladimirova, and M. Sweeting, "Image compression systems on board satellites," *Elsevier Acta Astronautica*, vol. 64, pp. 988–1005, 2009.

[4] I. 15444-1, *Information Technology—JPEG2000 Image Coding System, Part 1: Core Coding System*, ISO/IEC Std., 2000.

[5] S. Seo and M. Azimi-Sadjadi, "A 2-D filtering scheme for stereo image compression using sequential orthogonal subspace updating," *IEEE Trans. Circuits Syst. Video Technol.*, vol. 11, no. 1, pp. 52–66, 2002.

[6] D. Slepian and J. Wolf, "Noiseless coding of correlated information sources," *IEEE Trans. Inform. Theory*, vol. 19, pp. 471–480, Jul. 1973.

[7] A. Wyner and J. Ziv, "The rate-distortion function for source coding with side information at the decoder," *IEEE Trans. Inform. Theory*, vol. 22, pp. 1–10, Jan. 1976.

[8] Y. Wang, S. Rane, P. Boufounos, and A. Vetro, "Distributed compression of zerotrees of wavelet coefficients," in *Proc. ICIP-2011 IEEE International Conference on Image Processing*, 2011.

[9] A. Abrardo, M. Barni, E. Magli, and F. Nencini, "Error-resilient and low-complexity onboard lossless compression of hyperspectral images by means of distributed source coding," *IEEE Trans. Geoscience and Remote Sensing*, vol. 48, no. 4, pp. 1892–1904, 2010.

[10] S. Wang, L. Cui, and S. Cheng, "Adaptive Wyner-Ziv Decoding using Particle-based Belief Propagation," in *IEEE Globecom*, 2010.

[11] L. Stankovic, V. Stankovic, S. Wang, and S. Cheng, "Distributed Video Coding with Particle Filtering for Correlation Tracking," *Proc. EUSIPCO, Aalborg, Denmark*, 2010.

[12] S. Cheng and Z. Xiong, "Successive refinement for the Wyner-Ziv problem and layered code design," *IEEE Trans. Signal Processing*, vol. 53, no. 8, pp. 3269–3281, 2005.

[13] D. Varodayan, A. Mavlankar, M. Flierl, and B. Girod, "Distributed grayscale stereo image coding with unsupervised learning of disparity," in *IEEE Data Compression Conference*, 2007, pp. 143–152.

[14] Z. Xiong, A. Liveris, and S. Cheng, "Distributed source coding for sensor networks," *IEEE Signal Process. Magazine*, vol. 21, pp. 80–94, Sep. 2004.

[15] V. Stankovic, A. D. Liveris, Z. Xiong, and C. N. Georghiades, "On code design for the Slepian-Wolf problem and lossless multiterminal networks," *Information Theory, IEEE Transactions on*, vol. 52, no. 4, pp. 1495–1507, 2006.

[16] Y. Yang, V. Stankovic, Z. Xiong, and W. Zhao, "On Multiterminal Source Code Design," *Information Theory, IEEE Transactions on*, vol. 54, no. 5, pp. 2278–2302, 2008.

[17] R. Nagura, "Multi-stereo imaging system using a new data compression method," in *Proc. IGARSS-2006 IEEE International Geoscience and Remote Sensing Symposium*, 2006.

[18] A. Kiely, A. Ansar, A. Castano, M. Klimesh, and J. Maki, "Lossy image compression and stereo ranging quality from Mars rovers," *IPN Progress Report 42-168*, 2007.

[19] "Image compression algorithm altered to improve stereo ranging," *Tech Brifs, available at http://www.techbriefs.com/component/content/article/2673*, 2007.

[20] P. Meyer, R. Westerlaken, R. Gunnewiek, and R. Lagendijk, "Distributed source coding of video with non-stationary side-information," in *Proc. SPIE*, vol. 5960. Citeseer, 2005, pp. 857–866.

[21] M. Dalai, R. Leonardi, and F. Pereira, "Improving turbo codec integration in pixel-domain distributed video coding," in *Acoustics, Speech and Signal Processing, 2006. ICASSP 2006 Proceedings. 2006 IEEE International Conference on*, vol. 2. IEEE, pp. II–II.

[22] C. Brites and F. Pereira, "Correlation noise modeling for efficient pixel and transform domain Wyner–Ziv video coding," *Circuits and Systems for Video Technology, IEEE Transactions on*, vol. 18, no. 9, pp. 1177–1190, 2008.

[23] X. Fan, O. Au, and N. Cheung, "Adaptive correlation estimation for general Wyner-Ziv video coding," in *Image Processing (ICIP), 2009 16th IEEE International Conference on*. IEEE, 2009, pp. 1409–1412.

[24] X. Huang and S. Forchhammer, "Improved virtual channel noise model for transform domain Wyner-Ziv video coding," pp. 921–924, 2009.

[25] X. Artigas, J. Ascenso, M. Dalai, S. Klomp, D. Kubasov, and M. Ouaret, "The DISCOVER codec: architecture, techniques and evaluation," in *Picture Coding Symposium*. Citeseer, 2007.

[26] A. Aaron, S. Rane, and B. Girod, "Wyner-Ziv video coding with hash-based motion compensation at the receiver," in *IEEE ICIP'04*, vol. 5, 2005, pp. 3097–3100.

[27] G. Petrazzuoli, M. Cagnazzo, and B. Pesquet-Popescu, "Fast and efficient side information generation in distributed video coding by using dense motion representations," *EUSIPCO, Aalborg, Denmark*, 2010.

[28] D. Varodayan, Y. Lin, A. Mavlankar, M. Flierl, and B. Girod, "Wyner-Ziv coding of stereo images with unsupervised learning of disparity," in *Proc. Picture Coding Symp., Lisbon, Portugal*. Citeseer, 2007.

[29] D. Chen, D. Varodayan, M. Flierl, and B. Girod, "Distributed stereo image coding with improved disparity and noise estimation," in *IEEE ICASSP*, 2008, pp. 1137–1140.

[30] A. Zia, J. P. Reilly, and S. Shirani, "Distributed parameter estimation with side information: A factor graph approach," in *IEEE ISIT*, 2007, pp. 2556–2560.

[31] V. Toto-Zarasoa, A. Roumy, and C. Guillemot, "Maximum Likelihood BSC parameter estimation for the Slepian-Wolf problem," *IEEE Communications Letters*, vol. 15, no. 2, pp. 232–234, 2011.

[32] N. Gehrig and P. Dragotti, "Distributed compression of multi-view images using a geometrical coding approach," in *Proc. ICIP-2007*, 2007.

[33] X. Zhu, A. Aaron, and B. Girod, "Distributed compression for large camera arrays," in *Proc. SSP-2003*, 2003.

[34] A. Jagmohan, A. Sehgal, and N. Ahuja, "Compression of light-field rendered images using coset codes," in *Proc. 37th Asilomar Conference*

18

*on Signals, Systems, and Computers*, 2003.

[35] G. Toffetti, M. Tagliasacchi, M. Marcon, A. Sarti, S. Tubaro, and K. Ramchandran, "Image compression in a multi-camera system based on a distributed source coding approach," in *Proc. Eusipco-2005*, 2005.

[36] L. Stankovic, V. Stankovic, and S. Cheng, "Distributed compression: Overview of current and emerging multimedia applications," in *ICIP-2011 IEEE International Conference on Image Processing*. IEEE, 2011.

[37] C. Guillemot, F. Pereira, L. Torres, T. Ebrahimi, R. Leonardi, and J. Ostermann, "Distributed monoview and multiview video coding: basics, problems and recent advances," *IEEE Signal Processing Magazine*, vol. 24, no. 5, pp. 67–76, 2007.

[38] R. Zamir, S. Shamai, and U. Erez, "Nested linear/lattice codes for structured multiterminal binning," *IEEE Trans. Inform. Theory*, vol. 48, no. 6, pp. 1250–1276, 2002.

[39] V. Stankovic, A. D. Liveris, Z. Xiong, and C. N. Georghiades, "On code design for the Slepian-Wolf problem and lossless multiterminal networks," *IEEE Transactions on Information Theory*, vol. 52, no. 4, pp. 1495–1507, 2006.